Available online at www.sciencedirect.com

ScienceDirect

Solar Energy 111 (2015) 396–406

SOLAR ENERGY

www.elsevier.com/locate/solener

Conversion of parabolic trough mirror shape results measured in different laboratory setups

S. Meiser *, E. Lüpfert, B. Schiricke, R. Pitz-Paal

German Aerospace Center (DLR), Linder Höhe, 51147 Cologne, Germany

Received 16 June 2014; received in revised form 12 September 2014; accepted 14 September 2014
Available online 19 October 2014

Communicated by: Associate Editor L. Vant-Hull

Abstract

Shape accuracy of mirror panels for parabolic trough solar collectors has a significant impact on the optical performance of the collectors in a solar power plant and is therefore carefully assessed by test laboratories and manufacturers. Relevant deformation is induced by gravity or mounting forces, so that shape accuracy data measured in different setups cannot be compared.

This paper presents a method for conversion of shape measured in a vertical laboratory setup into data for a horizontal laboratory setup. Characteristic deformation matrices for parabolic trough mirror panels of RP3 geometry are determined by deflectometric shape measurements on various mirror panels and by validated finite element analyses (FEA).

The resulting root mean square (rms) of measured slope deviation difference (i.e. the gravity induced deformation) between vertical and horizontal setup is on average 2.4 mrad for inner mirrors and 1.25 mrad for outer mirrors loosely positioned on a frame.

Measured data from vertical setup, transformed by such characteristic deformation matrices into horizontal shape results, differ by less than 0.2 mrad in rms slope deviation value from data measured in horizontal setup. Whereas the presented approach to convert shape accuracy measurement results is suitable for the calculation of rms values, some of the analyzed mirror samples show differences in local slope deviation values larger than the deflectometric measurement uncertainty. The amount of deviation depends on details of the accuracy of the positioning of the mirrors on the measurement frame and is affected by the fixation and associated mounting forces at the pads.

Keywords: Parabolic trough; Mirror shape; Deflectometry; Finite element analysis

1. Introduction

Shape accuracy of the mirror panels for parabolic trough collectors is a key parameter for optical performance that directly impacts the efficiency of a solar power plant. The high quality of state of the art mirror panels is ensured by measurements performed by independent test laboratories as well as by quality control in series production (Ulmer et al., 2012). Examples of common measurement techniques include the Video Scanning Hartmann Optical Test (VSHOT) developed by Sandia and NREL (Jones et al., 1997), visual inspection systems by ENEA (Montecchi and Maccari, 2007; Montecchi et al., 2011), and fringe reflection or deflectometry techniques by ISE (Burke et al., 2013), Sandia (Andraka et al., 2013) and DLR (März et al., 2011; Ulmer et al., 2011).

Measurement boundary conditions are not yet standardized and the shape measurements are performed in different setups that, for example, differ in measurement position. Previous work (Meiser, 2014; Meiser et al., 2014) quantifies the differences in shape accuracy results

* Corresponding author. Tel.: +49 2203 601 3978.
E-mail address: siw.meiser@dlr.de (S. Meiser).

http://dx.doi.org/10.1016/j.solener.2014.09.021
0038-092X/

Nomenclature

a_{ij}	surface element area projected into the collector aperture plane (m^2)
A_{tot}	total collector aperture area orthogonal to the optical axis (m^2)
$\vec{n}$	ideal surface normal vector
$\vec{n}_+, \vec{n}_-$	actual surface normal vectors
sdx_{ij}	local slope deviation (mrad)
SDx	root mean square slope deviation in transversal (x) direction (mrad)
SDy	root mean square slope deviation in longitudinal (y) direction (mrad)
u	combined standard uncertainty of slope deviation (mrad)
$\bar{u}$	mean combined standard uncertainty of slope deviation (mrad)
x, y, z	coordinate axes

Subscripts

calc	calculated
comp	computed (by means of finite element analysis)
h, v	horizontal, vertical
f, l	fix, loose
meas	measured (by deflectometry)
n	upper bound of summation
rms	root mean square

between the most common measurement setups for parabolic trough mirror panels and identifies measurement position, mounting mode and support frame employed for the measurement as relevant boundary conditions. If these boundary conditions deviate from one setup to the other, shape accuracy results cannot be compared. Moreover, shape quality specifications cannot be guaranteed to be met in different measurement conditions.

This paper presents a method to convert results obtained in different laboratory setups that allows the comparison of shape accuracy results. The examined setups are a vertical (mounting points vertically and curved direction horizontally aligned) and a horizontal measurement position (mirrors facing upward with mounting points horizontally aligned). Two cases are evaluated in both setups: the mirror tightened with screws to a support frame (fix case) and the mirror not tightened (loose case). The analyses are carried out for mirrors of RP3 geometry (focal length 1.71 m, trough aperture width 5.78 m, panel length 1.7 m) which is the most commonly employed mirror type in current parabolic trough power plant projects. Characteristic gravity-induced deformation and resulting slope deviation difference matrices are determined from measurement results obtained at the deflectometry test bench at DLR's Test and Qualification Center (QUARZ® Center) in Cologne and finite element analyses. They are added to vertically measured data to calculate horizontal results. The calculated results are compared to measured results in order to evaluate the accuracy of the suggested method. The finite element models prepared for this study are additionally validated.

2. Methodology

2.1. General definitions and description of reflector panels of RP3 geometry

In collectors that employ reflector mirrors of RP3 geometry the parabolic shape is formed by two inner and two outer mirror panels having dimensions of 1641 × 1700 mm (RP3 inner mirror) and 1501 × 1700 mm (RP3 outer mirror). They are made of 4 mm thick bent float glass sheets. Four ceramic mounting pads are glued to the mirror rear side for mounting it onto the collector support structure.

By definition, the point of origin of the according coordinate system is located in the parabola vertex (compare Fig. 1). The z-axis points from the vertex of the parabola towards the focal line. The y-axis runs parallel to the symmetry axis of the parabola and the x-axis points in the direction of mirror curvature.

Slope deviation is a measure for the shape accuracy of a mirror panel. Slope deviation values are typically measured spatially resolved and are defined as the angle between actual surface normal ($\vec{n}_+$ or $\vec{n}_-$, compare Fig. 1, right) and ideal surface normal $\vec{n}$. An outward rotation of the deformed surface normal vector relative to the original surface normal vector is defined as positive slope deviation value, an inward rotation as a negative value. By definition, the outward direction points to the outer edges of the parabolic trough, the inward direction toward the center of the trough.

Since gravity-induced deformation in non-curved (y) direction is less pronounced (Meiser, 2014) and the impact of slope deviation in y-direction on the intercept factor is of factor 10 lower than in curved (x) direction (Lüpfert and Ulmer, 2009), this study focuses on the evaluation of slope deviation values in x-direction.

2.2. Measurement of mirror shape accuracy and measured characteristic deformation

Deflectometry (also: fringe reflection) is an accurate and fast technique to measure shape accuracy of reflective surfaces with high resolution. A software algorithm uses the images of regular stripe patterns that are reflected and distorted by the surface to calculate local slope deviation values.

Reflector shape accuracy is furthermore evaluated in terms of standard deviation parameters of the reflector

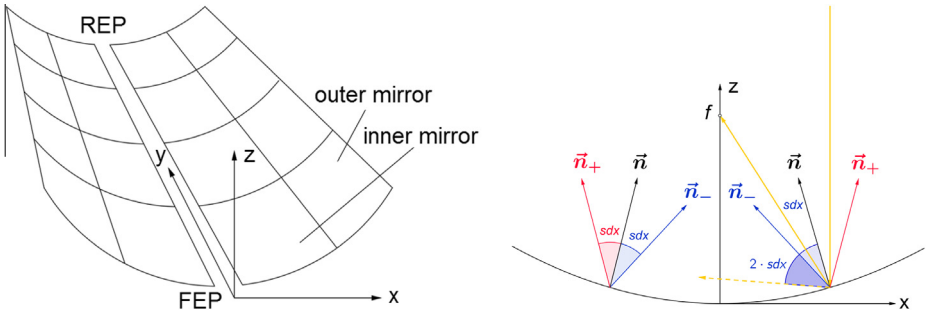

Fig. 1. Left: coordinate system of a parabolic trough collector module (REP: rear end plate, FEP: front end plate); right: definition of slope deviation in curved (x) direction sdx and ideal and actual surface normal vectors, $\vec{n}$ and $\vec{n}_+, \vec{n}_-$ (yellow arrows represent incoming and reflected solar radiation). (For interpretation of the references to colour in this figure legend, the reader is referred to the web version of this article.)

slope of the whole mirror panel. Root mean square (rms) slope deviation values are calculated based on the area-weighted local slope deviation values. Typically, these parameters are evaluated in both x and y (transversal and longitudinal) directions of the trough collector, SDx and SDy, respectively. For example, in transversal, curved (x) direction rms slope deviation is defined as

$$SDx = \sqrt{\sum_{i,j=1}^{n} \left(sdx_{ij}^2 \cdot \frac{a_{ij}}{A_{tot}} \right)} \tag{1}$$

with local slope deviation values sdx_{ij}, the according surface element areas a_{ij} projected into the aperture plane and the total aperture area A_{tot}.

The deflectometric measurement method is described in more detail in Ulmer et al. (2008). März et al. (2011) give a standard uncertainty of 0.2 mrad for the rms value of measured slope deviation. According to the Gaussian law of propagation of uncertainty, the standard uncertainty of the rms of local slope deviation differences is

$$u(SDx_{h-v}) = \sqrt{u^2(SDx_h) + u^2(SDx_v)} = \sqrt{0.2^2 + 0.2^2}\,\text{mrad} = 0.28\ \text{mrad}. \tag{2}$$

The mean combined standard uncertainty of local slope deviation values for the test bench at the QUARZ® Center is $\bar{u}(sdx) \leq 0.7$ mrad (Meiser, 2014).

Common measurement setups in laboratory are:

- Vertical loose setup (*vl*): vertical measurement position without tightening of screws, mounting pads are vertically and curved (x) direction is horizontally aligned, mirror is carefully leaned against an ideally aligned support frame so that deformation due to dead load is negligible.
- Horizontal loose setup (*hl*): horizontal measurement position without tightening of screws, mounting pads are horizontally aligned, the mirror faces upward and is placed onto an ideally aligned support frame.
- Vertical fix setup (*vf*): mirror oriented as in vertical loose measurement setup, mirror mounting pads are fixed to a support frame with screws (can only be realized for mirrors with attached mounting pads).
- Horizontal fix setup (*hf*): mirror oriented as in horizontal loose measurement setup, mirror mounting pads are fixed to a support frame with screws (can only be realized for mirrors with attached mounting pads).

It should be noted that the "vertical" setup in laboratory does not correspond to any orientation achieved during collector operation. However, since it allows assessing shape accuracy without the influence of gravity, it may provide valuable information with regard to the improvement of the manufacturing process.

The employed laboratory support frame is constructed of aluminum beams and is equipped with precisely manufactured steel supports. The alignment of the supports is checked in terms of height, distances and angles using steel rulers, try square, digital sliding caliper and high precision electronic inclinometer.

The deflectometric test bench at DLR's QUARZ® Center is employed to measure mirror shape accuracy in all four setups for a total of eleven annealed sag-bent RP3 inner mirror panels of three different production periods, twelve annealed sag-bent RP3 outer mirror panels of three different production periods and five tempered press-bent RP3 outer mirror panels of one production period.

The measurement data is evaluated for the whole mirror area without neglecting a rim.

In order to determine the characteristic deformation from vertical to horizontal orientation, the difference from vertical to horizontal position in slope deviation in x-direction is evaluated for each mirror panel. The slope deviation difference data is averaged for all evaluated inner and outer panels, respectively, to determine the characteristic measured deformation matrix, e.g. for fixed mounting mode $\overline{\left(sdx_{hf_{ij}} - sdx_{vf_{ij}}\right)}_{\text{meas}}$.

2.3. Finite element analyses and computed deformation

Characteristic computed deformation matrices are determined in finite element analyses of perfect parabolic mirrors and laboratory support frame. Two different model cases for each mirror type are prepared in ANSYS Workbench, one with the mirror tightened with screws to the

support frame (fix cases), the other without tightening the mirror (loose cases).

It is assumed that the reflective and protective coatings do not affect the deformation behavior of the mirrors so that they are neglected in the models. The mounting pads are modeled as solid ceramic cylinders. The analyses use real material properties. Small parts (screws, screw nuts, etc.) are not included in the models. Real joints are not modeled, all parts are fixed permanently. Because the reflector mirrors are thin, they are discretized utilizing solid shell elements. Solid elements are used for the modeling of adhesive, pads, brackets and further parts of the support frame.

The *fix model cases* consist of the inner or outer reflector mirror mounted onto the laboratory support frame that is equipped with precisely manufactured steel supports. Fixed boundary conditions are applied to the rear side of the bottom of the frame's aluminum beams. Fixed boundary conditions constrain all degrees of freedom on the mounting pads' rear sides so that there is neither displacement nor rotation possible at those locations (Fig. 2).

The *loose model cases* do not include the support frame in the model but consider its deformation if the respective mirror is mounted onto the frame. The displacement values of the support frame on the mounting pads' rear side resulting in the fix laboratory case are applied to the rear side of the mounting pads (remote displacement boundary condition). Rotation around the support points is allowed (Fig. 2).

The static structural analyses consider only linear elastic deformation of the models and are run in horizontal laboratory position.

The computed displacement data serve for calculation of local and rms slope and focus deviation values in x-direction. Further details of the finite element models are given in Meiser (2014).

In order to validate the finite element models the slope deviation data resulting from the measured and modeled deformation are compared. The models can be considered accurate if the predicted slope deviation values are within the uncertainty of the deflectometric measurement system.

2.4. Conversion of results

For a conversion of measurement results from vertical to horizontal laboratory position the according measured characteristic deformation matrix $\overline{\left(sdx_{hf_{if}} - sdx_{vf_{ij}}\right)}_{\text{meas}}$ is added to spatially resolved measured slope deviation values in transversal (x) direction of a vertical measurement position $sdx_{v,meas_{ij}}$ to calculate spatially resolved results $sdx_{h,calc_{ij}}$ corresponding to a horizontal measurement position, i.e. for fixed mounting mode:

$$sdx_{hf,calc_{ij}} = sdx_{vf,meas_{ij}} + \overline{\left(sdx_{hf_{ij}} - sdx_{vf_{ij}}\right)}_{meas} \tag{3}$$

In a second analysis horizontal results are calculated by adding the deformation matrix $\left(sdx_{hf_{ij}} - sdx_{vf_{ij}}\right)_{comp}$ that is computed in a finite element analysis (FEA) to spatially resolved vertically measured slope deviation values:

$$sdx_{hf,calc_{ij}} = sdx_{vf,meas_{ij}} + \left(sdx_{hf_{ij}} - sdx_{vf_{ij}}\right)_{comp} \tag{4}$$

Root mean square values of slope deviation are then calculated according to Eq. (1). The root mean square values as well as spatially resolved slope deviation in x-direction for measured and calculated horizontal position are compared. It is assessed additionally whether the procedure of adding measured or the procedure of adding computed deformation matrices to vertical results better predicts horizontal results.

3. Results

3.1. Measured mirror shape accuracy in different laboratory positions and mounting modes

Fig. 3 illustrates how measurement position and mounting mode may affect the measured shape accuracy result. Spatially resolved measured slope deviation values of one

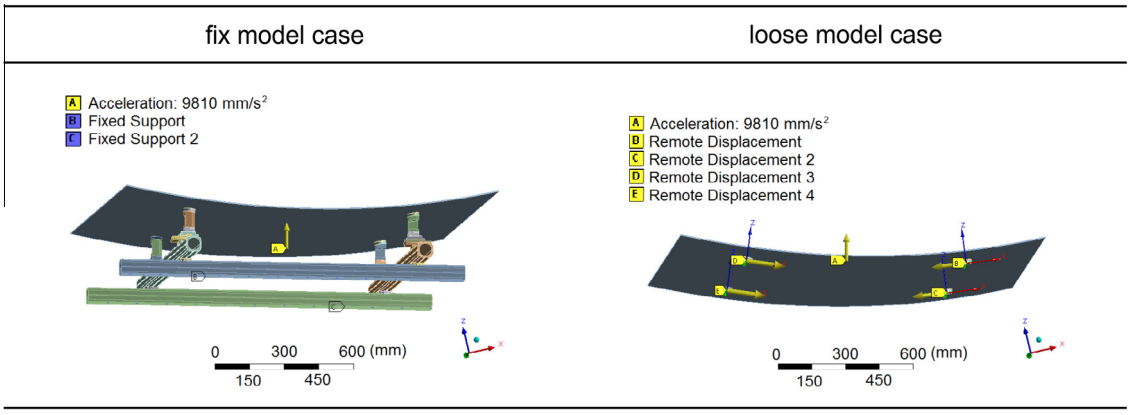

Fig. 2. ANSYS model of an ideally shaped RP3 inner mirror panel, fixed onto a laboratory support structure (fix model case) and placed onto a laboratory support frame without fixation (loose model case).

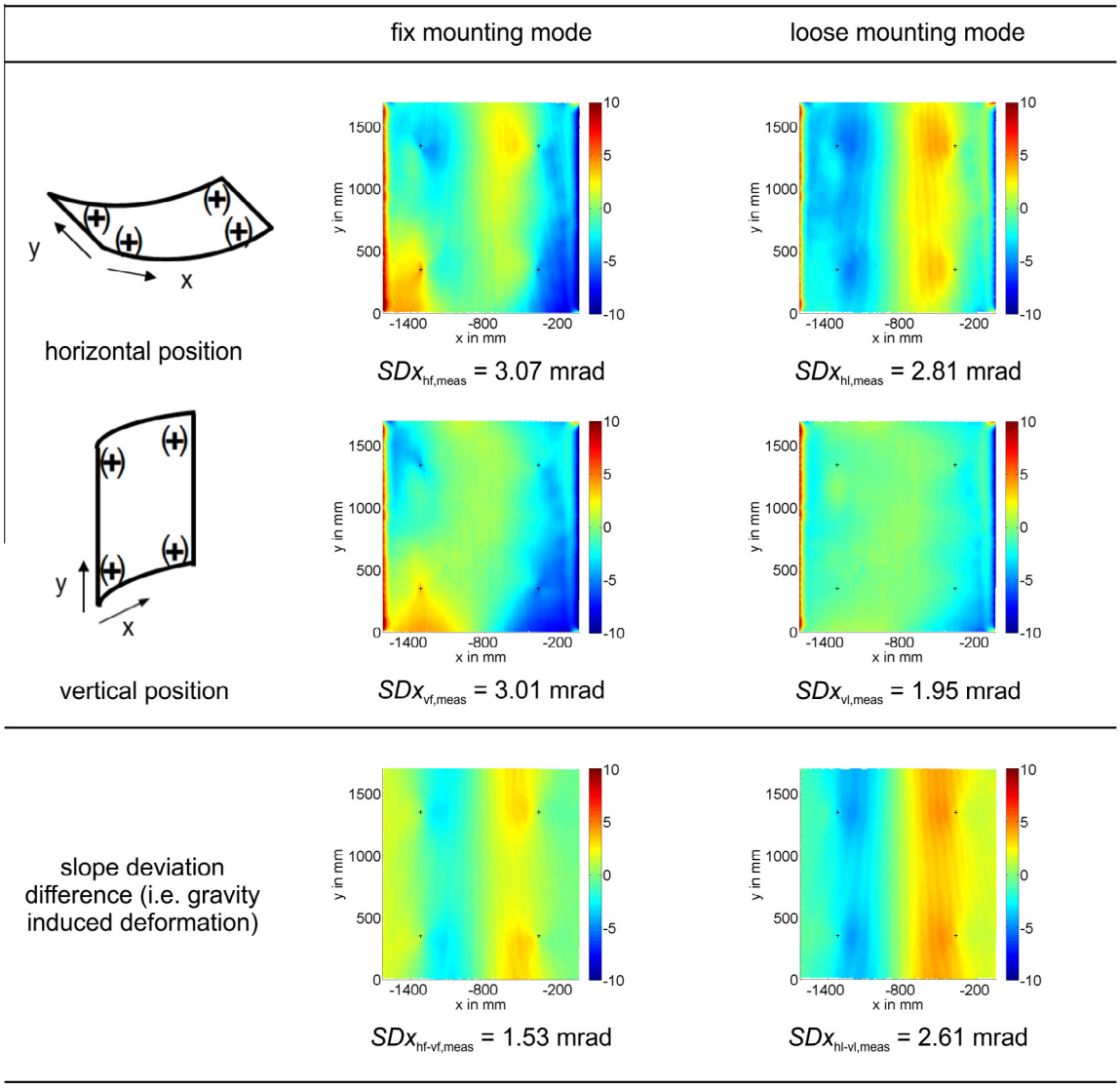

Fig. 3. Slope deviation in mrad in x-direction for an exemplary annealed sag-bent RP3 inner mirror panel in horizontal (top) and vertical laboratory measurement position (middle) and the difference in slope deviation between the two positions (bottom).

exemplary RP3 inner mirror panel in all four measurement setups as well as the according slope deviation difference between horizontal and vertical measurement position is depicted.

The mirror panel sags inward between the mounting points from vertical to horizontal position for both fixed and loose mounting modes, while the extent of the sag along the non-curved mirror edges depends on the mounting mode. The inward sag between the mounting points is indicated by positive slope deviation difference values (see bottom of Fig. 3) in the x-range from the center of the mirror to the inner mounting points and negative slope deviation difference values in the x-range from the center towards the outer mounting points. In case of fixed mounting, the non-curved mirror edges deflect downwards. The loose measurement setup allows a rotation of the mirror about the support points so that the non-curved mirror edges deflect upwards.

The comparison of vertical measurement results in Fig. 3 demonstrates the influence of a further factor on measured shape accuracy. In case of angularly deviating mounting pads a significant difference of local slope deviation values between mirrors evaluated in a setup fixed and mirrors evaluated in a setup not fixed to a support frame may appear.

Fig. 4 shows the characteristic gravity-induced slope deviation differences for the measured RP3 mirror panels that were obtained by averaging measured slope deviation differences. If mirrors are fixed to the support frame the measured root mean square slope deviation difference is on average 1.5 mrad and 1.1 mrad (compare Fig. 4) for inner and outer mirror respectively. Gravity-induced deformation is more pronounced for the loose mounting mode. In this case, measured rms slope deviation difference is on average 2.4 mrad for inner mirror panels and 1.3 mrad for outer mirror panels (compare Fig. 4).

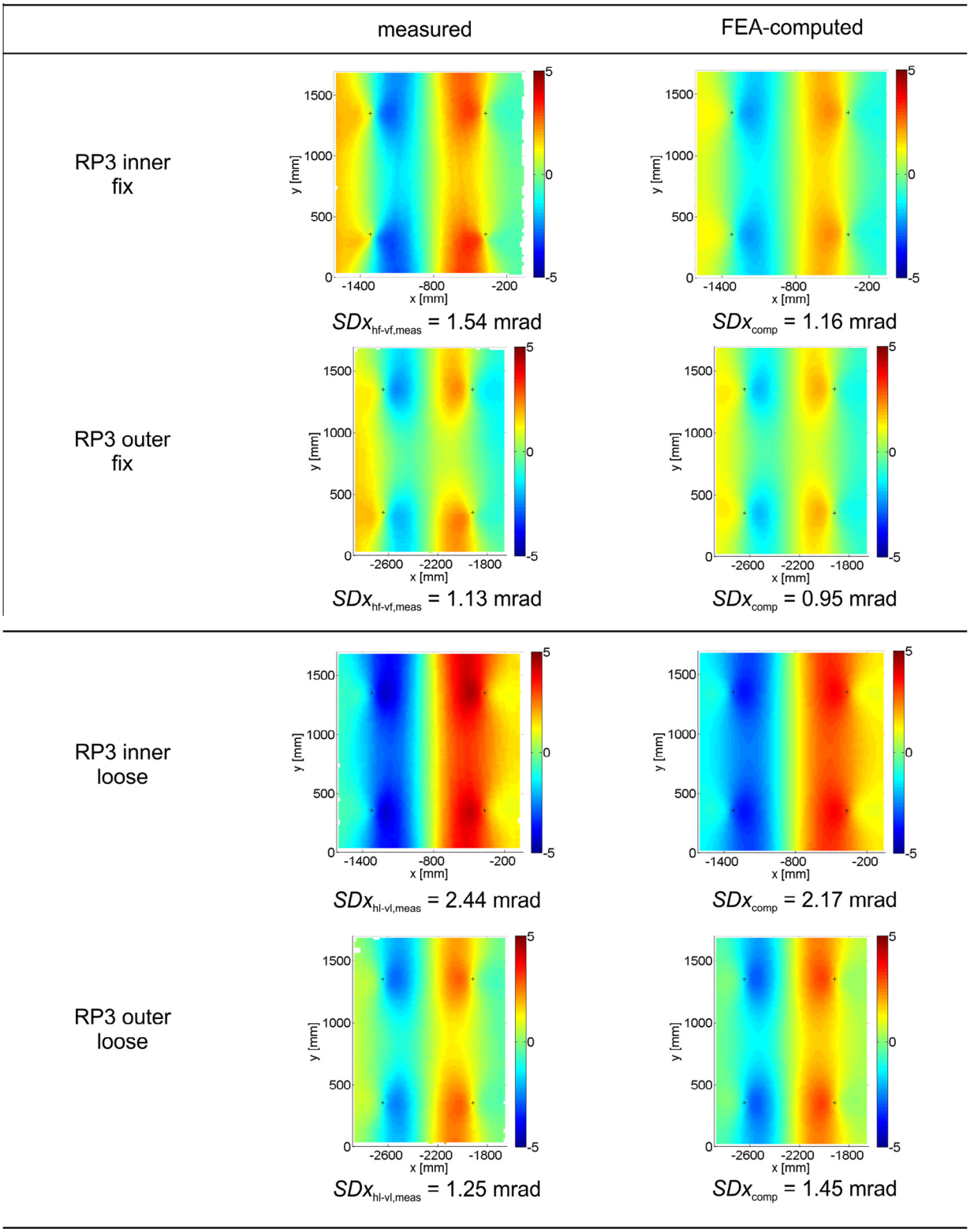

Fig. 4. Deformation matrices horizontal-vertical setup: Measured and FEA-computed slope deviation differences for the fix laboratory model case (top) and for the loose laboratory model case (bottom) for a RP3 inner and a RP3 outer panel respectively. Color bars in mrad and in ±5 mrad range for reasons of increasing informative value. FEA-computed results are described in the next section. (For interpretation of the references to color in this figure legend, the reader is referred to the web version of this article.)

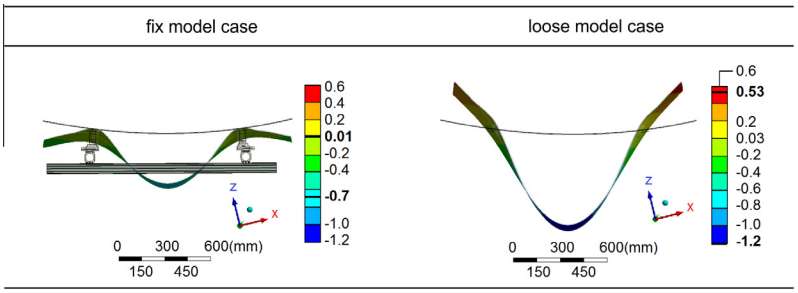

Fig. 5. Gravity-induced deformation of an ideally shaped RP3 inner mirror panel for fix and loose mounting mode in horizontal laboratory position. Scaling factor of deformation graphics: 500.

Due to the smaller distance between mounting pads for RP3 outer mirrors, deformation and hence slope deviation differences are smaller for RP3 outer mirrors. The deformation matrices obtained by finite element analyses (right column of Fig. 4) are described in the next section.

3.2. Finite element analyses and computed deformation

Fig. 5 displays gravity-induced deformation of a RP3 inner mirror in horizontal laboratory position. As clearly indicated in the deformation side view graphics the chosen setup determines the typical deformation characteristic. Compared to the non-deformed model which is sketched as black line in the figures, the mirrors show a symmetrical "M"-shaped deformation in curved direction when fixed with screws to a laboratory support frame. If the mirrors are not tightened with screws they are allowed to rotate about the mounting points leading to a "V"-shaped gravity-induced deformation characteristic.

In order to validate the finite element models, the resulting spatially resolved gravity-induced slope deviation values are compared to the according measured slope deviation differences in Fig. 4. As indicated by the consistent color gradients in the graphics, the finite element analyses very well predict slope deviation differences between horizontal and vertical setup.

However, the fix laboratory model cases slightly underestimate gravity-induced deformation which may be due to the underlying assumptions. The finite element models, for example, neglect small parts (screws, screw nuts, etc.) and assume that all parts connected by screws are fixed permanently. In reality, those bolted connections might allow for a marginal movement.

If the rms values are compared it can be stated that the computed gravity-induced rms slope deviation values are within an extended uncertainty interval of the stated uncertainty for measured rms slope deviation differences of $2 \cdot u(SDx_{h-v}) = 2 \cdot 0.28\ \text{mrad} = 0.56\ \text{mrad}$. Except for the calculated root mean square value of the inner mirror in the fix laboratory model case the root mean square values are even within the 1σ uncertainty interval given by the determined standard uncertainty.

3.3. Conversion of results: vertical to horizontal

Figs. 6 and 7 compare spatially resolved slope deviation values in x-direction that were measured in horizontal laboratory position at DLR's test bench with values that were calculated by adding the according measured (Fig. 6) or FEA-computed (Fig. 7) deformation matrices to vertically measured slope deviation values.

Similar color distributions in measured and calculated graphical results indicate a very good agreement of measured and calculated local slope deviation values. The maps showing the differences in local values reveal local deviations that are higher than ± 1 mrad and thus are larger than the stated standard uncertainty for measured local slope deviation values of $\leqslant 0.7$ mrad (Meiser, 2014). The fine stripe patterns in the difference graphics of the RP3 inner mirrors are an artifact of the measurement system. If a slight variation in the background light occurs during the measurement, the finest stripe patterns used for coding of the target surface become visible in the difference graphics (measured-calculated) with enlarged scale.

The slight differences in measured rms slope deviation values in Figs. 6 and 7 are due to the different resolutions of original measurement results (Fig. 6) and measurement results with reduced resolution (Fig. 7). In order to calculate horizontal results by adding the computed deformation matrix, the resolution of the measurement results have to be reduced to the resolution of the finite element model. The lower resolved measurement results are then compared to calculated results.

Tables 1 and 2 summarize the mean differences between measured and calculated root mean square values for all examined mirrors $\overline{SDx_{hf/l,meas} - SDx_{hf/l,calc}}$ and the mean rms values of local differences in slope deviation $\overline{SDx_{hf/l,meas-calc}}$ for results obtained by adding the measured or FEA-computed deformation matrices respectively. The mean differences between measured and calculated root mean square values are all below 0.18 mrad. However, the mean rms values of local difference in slope deviation $\overline{SDx_{hf/l,meas-calc}}$ are at most as high as 0.34 mrad if measured deformation matrices are added and at most as high as 0.6 mrad if computed deformation matrices are used to convert the results. The values of $\overline{SDx_{hf/l,meas-calc}}$ are a

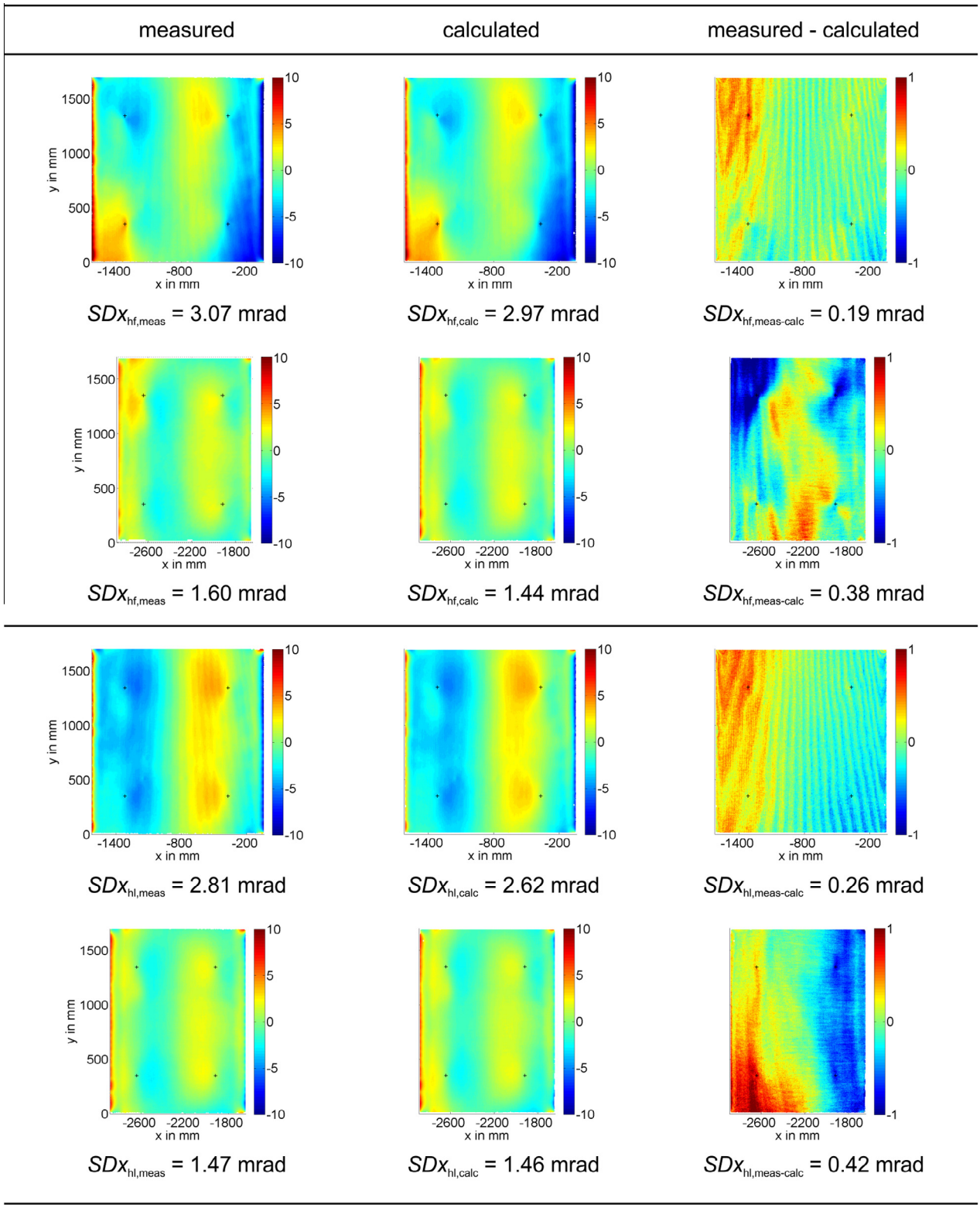

Fig. 6. Measured and calculated slope deviation in horizontal fix (top) and horizontal loose (bottom) measurement position for exemplary RP3 inner and outer mirror panels. Calculated results are obtained using *measured slope deviation differences*. Color bars in mrad. (For interpretation of the references to color in this figure legend, the reader is referred to the web version of this article.)

measure for local differences between measured and calculated slope deviation. They are slightly higher for results that were calculated using computed deformation matrices due to the assumptions made for the finite element analyses (neglect of small parts and assumption that all parts connected by screws are fixed permanently).

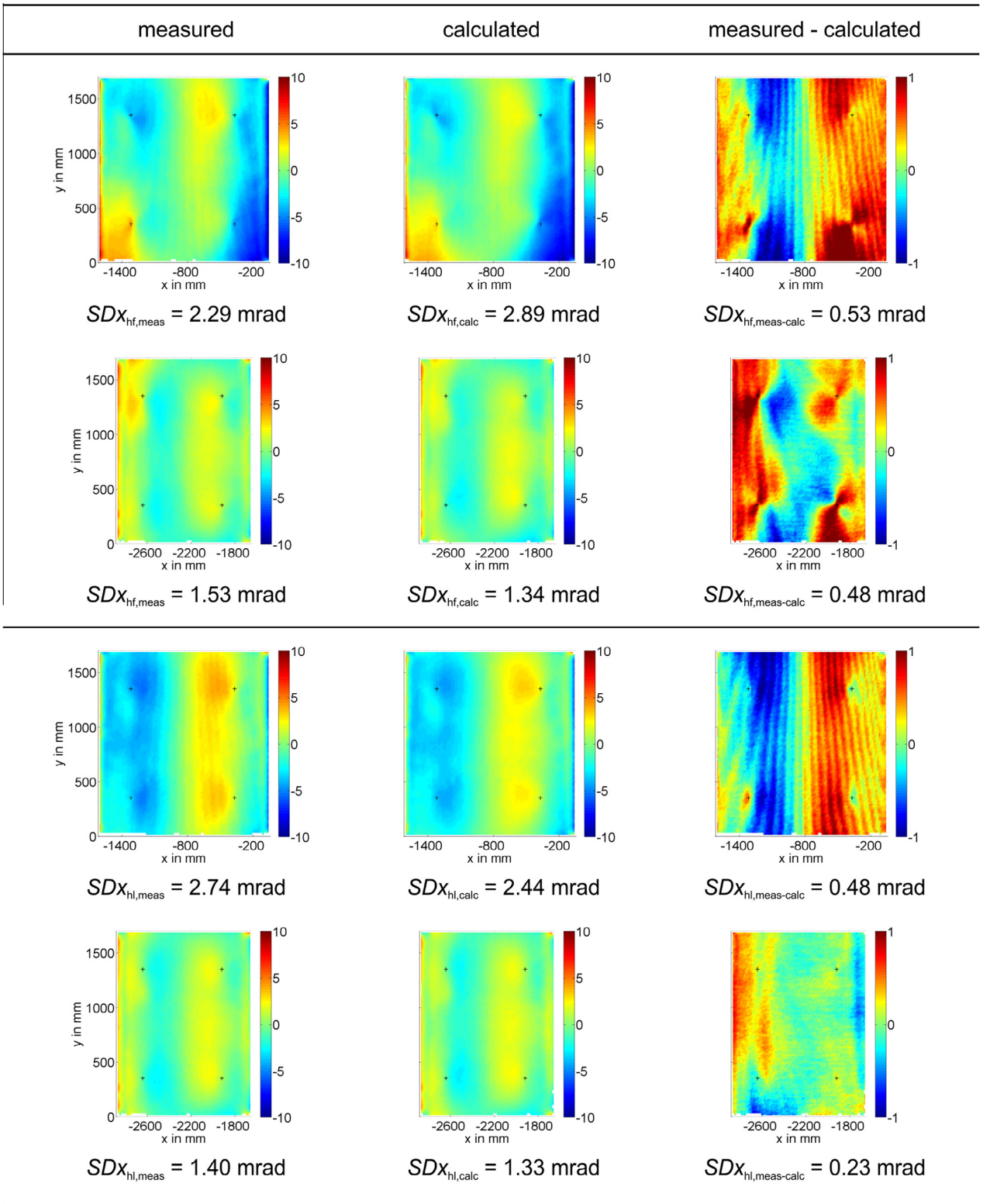

Fig. 7. Measured and calculated slope deviation in horizontal fix (top) and horizontal loose (bottom) measurement position for exemplary RP3 inner and outer mirror panels. Calculated results are obtained using *FEA-computed slope deviation differences*. Color bars in mrad. (For interpretation of the references to color in this figure legend, the reader is referred to the web version of this article.)

Table 1
Mean differences between measured and calculated rms slope deviation values and mean rms value of local slope deviation differences of all examined RP3 inner and outer mirror panels for fix (top) and loose (bottom) mounting mode. Calculated results are obtained using *measured slope deviation differences*. All values in mrad.

	$\overline{\lvert SDx_{hf,meas} - SDx_{hf,calc}\rvert}$	$\overline{SDx_{hf,meas-calc}}$
RP3 inner	0.14	0.26
RP3 outer	0.10	0.26
	$\overline{\lvert SDx_{hl,meas} - SDx_{hl,calc}\rvert}$	$\overline{SDx_{hl,meas-calc}}$
RP3 inner	0.12	0.29
RP3 outer	0.09	0.34

Table 2
Mean differences between measured and calculated rms slope deviation values and mean rms value of local slope deviation differences of all examined RP3 inner and outer mirror panels for fix (top) and loose (bottom) mounting mode. Calculated results are obtained using *FEA-computed slope deviation differences*. All values in mrad.

	$\overline{\lvert SDx_{hf,meas} - SDx_{hf,calc}\rvert}$	$\overline{SDx_{hf,meas-calc}}$
RP3 inner	0.13	0.60
RP3 outer	0.08	0.42
	$\overline{\lvert SDx_{hl,meas} - SDx_{hf,calc}\rvert}$	$\overline{SDx_{hl,meas-calc}}$
RP3 inner	0.18	0.47
RP3 outer	0.12	0.50

4. Discussion

The presented approach to convert shape accuracy measurement results achieved in vertical measurement position into results applying for the horizontal position by adding the characteristic slope deviation difference matrices is suitable for the calculation of root mean square values. For the studied mirror panels the mean difference between measured and calculated rms slope deviation is smaller than the standard uncertainty of 0.2 mrad for the rms value of measured slope deviation. As indicated by higher mean rms values of local slope deviation differences, the conversion of results is a little less accurate if characteristic deformation matrices are determined by finite element analyses.

Results for some of the analyzed mirror samples show local differences between measured and calculated local slope deviation values that are higher than the stated standard uncertainty for measured local slope deviation values of $\leqslant 0.7$ mrad. This is mainly due to the facts that the vertical measurement position is susceptible to positioning inaccuracies and that possible interaction of angularly deviating mounting pads with the support frame were neglected in this study.

As analyzed in Meiser et al. (2014), the geometry and rigidity of the support frame relevantly influences the measured shape accuracy results. Thus, the difference matrices that were identified in this study employing deflectometric measurements and finite element analyses are not transferable to setups that use support frames of different geometry and rigidity. In that case the shape accuracy measurements would have to be repeated or finite element analyses including the modified support frame would have to be carried out in order to determine the respective characteristic deformation matrices.

If measurements are performed in horizontal position, the vertical results can be determined by reversing the procedure, i.e. deformation matrices are subtracted from horizontal results to obtain vertical results. Moreover, slope deviation in further orientations can be calculated by adding the according difference matrices to vertical results. The calculation of further shape accuracy parameters, such as focus deviation, can be carried out using the determined slope deviation values.

A conversion of shape accuracy results achieved in horizontal loose position (e.g. if uncoated glass panels are evaluated) into horizontal fix results has to take into account an additional calculation step in order to account for a possible angular deviation of the mounting pads. The significant influence of the angular deviation of mounting pads on shape accuracy results is studied separately in detail in Meiser (2014).

5. Conclusion

The preliminary study of shape accuracy in different setups demonstrates significant gravity-induced mirror deformation and resulting differences in shape accuracy results for different measurement positions and mounting modes. Consequently, when performing measurements of this kind, these measurement parameters should be stated in addition to the measurement result.

A method to convert mirror shape accuracy results of parabolic trough mirror panels obtained in different measurement positions based on measurements and finite element analyses is presented and assessed.

Measurement data and finite element analyses results serve for determination of characteristic mirror deformation from vertical to horizontal laboratory measurement setup for mirrors tightened with screws to a support frame as well as for mirrors not tightened to a frame. The resulting slope deviation values are found to be in the magnitude of shape quality of state of the art mirror panels. The finite element models calculate gravity-induced mirror deformation and resulting slope deviation with acceptable accuracy.

A conversion of results from vertical to horizontal measurement position is achieved by first, adding measured slope deviation difference values and second, by adding computed slope deviation values identified in finite element analyses. The comparison of horizontally measured and calculated results reveals that a conversion is possible regarding the calculation of root mean square slope deviation values. Some of the analyzed mirror samples show differences between measured and calculated local slope deviation values that are locally higher than ± 1 mrad and thus larger than the standard uncertainty of the deflectometric measurement method.

Collector support structures to which the mirrors are mounted for operation are different from the laboratory frame presented in this paper and may differ from one collector to the other. However, if the mounting conditions and the mechanical properties of the support structure are known the presented methodology allows to reliably predict mirror shape accuracy in various operating orientations by adding the according deformation matrices. These results can serve as input data for further ray tracing analyses to determine optical collector performance in all tracking angles, to draw conclusions concerning a representative measurement setup for which the specifications for mirror shape have to be met and to identify possible optimization approaches.

Acknowledgements

The financial support for part of this work by FLABEG FE GmbH in the framework of a cooperation project is gratefully acknowledged.

References

Andraka, C.E., Sadlon, S., Myer, B., Trapeznikov, K., Liebner, C., 2013. Rapid reflective facet characterization using fringe reflection techniques. J. Sol. Energy Eng. 136, 011002–011002.

Burke, J., Li, W., Heimsath, A., von Kopylow, C., Bergmann, R.B., 2013. Qualifying parabolic mirrors with deflectometry. J. Europ. Opt. Soc. Rap. Public. 8, 13014.

Jones, S.A., Gruetzner, J.K., Houser, R.M., Edgar, R.M., Wendelin, T.J., 1997. VSHOT Measurement Uncertainty and Experimental Sensitivity Study. In: Proceedings of the 32nd Intersociety Energy Conversion Engineering Conference – IECEC, pp. 1877–1882.

Lüpfert, E., Ulmer, S., 2009. Solar Trough Mirror Shape Specifications. In: Proceedings of the 15th SolarPACES Conference, Berlin (Germany).

März, T., Prahl, C., Ulmer, S., Wilbert, S., Weber, C., 2011. Validation of two optical measurement methods for the qualification of the shape accuracy of mirror panels for concentrating solar systems. J. Sol.Energy Eng. 133, 031022.

Meiser, S., 2014. Analysis of Parabolic Trough Concentrator Mirror Shape Accuracy in Laboratory and Collector. PhD thesis, RWTH Aachen University, Germany.

Meiser, S., Lüpfert, E., Schiricke, B., Pitz-Paal, R., 2014. Analysis of parabolic trough concentrator mirror shape accuracy in different measurement setups. Energy Procedia 49, 2135–2144.

Montecchi, M., Maccari, A., 2007. An optical profilometer for the characterisation of parabolic trough solar concentrators. Sol. Energy 81, 185–194.

Montecchi, M., Benedetti, A., Cara, G., 2011. Fast 3D Optical-Profilometer for the Shape-Accuracy Control of Parabolic-Trough Facets. In: Proceedings of the 17th SolarPACES Conference, Granada (Spain).

Ulmer, S., Heller, P., Reinalter, W., 2008. Slope measurements of parabolic dish concentrators using color-coded targets. J. Sol.Energy Eng. 130, 011015.

Ulmer, S., März, T., Prahl, C., Reinalter, W., Belhomme, B., 2011. Automated high resolution measurement of heliostat slope errors. Sol. Energy 85, 681–687.

Ulmer, S., Weber, C., Koch, H., Schramm, M., Pflüger, H., Climent, P., Yildiz, H., 2012. High-Resolution Measurement System for Parabolic Trough Concentrator Modules in Series Production. In: Proceedings of the 18th SolarPACES Conference, Marrakech (Morocco).